

Non-Hamiltonian Transverse-Longitudinal Emittance Transfer in Circular Accelerators

Lajos Bojtár*
CERN, CH-1211 Genève 23

(Dated: April 15, 2022)

The usual configuration of electromagnetic fields used in accelerators give rise to systems which can be described by Hamiltonian mechanics. If the beam is transferred in a symplectic and linear manner a continuous emittance transfer between different planes of motion is not possible, only a complete exchange. Continuous transfer in many cases would be useful. In this paper we present a new method to achieve a continuous transfer between transverse and longitudinal planes using a transverse quadrupole RF electric field, generated by an RFQ like resonant device. The electric field generated by the resonator is non-conservative. The resulting system is non-Hamiltonian and the constraints of the Hamiltonian systems don't apply. Tracking studies with single particles and 6D Gaussian bunches has been performed. The new method might lead to significant transverse emittance decrease in accelerators and luminosity increase in colliders.

I. INTRODUCTION

In accelerators one of the most important parameter of a particle beam is its emittance, in many cases reducing the emittance is highly important. The common method to achieve small emittance is beam cooling. Cooling methods reduce the volume of the 6 dimensional phase-space. There are several types of cooling methods, each having its limitations, and in many cases non of those method can be used, or they are not practical. In certain cases is more important to have small emittance in one or two planes of motion than the others. In these cases a transfer of emittance between the planes can lead to significant performance improvements. Currently known methods [1], [2] for complete emittance exchange between subspaces are subjects to certain restrictions. In accelerators where the beam transfer is symplectic and linear there are constraints which prevents the continuous transfer of emittances between different planes of motion, only a complete exchange is possible. This was first proved by E.D Courant [3] and it is known as the emittance exchange theorem [4]. An other method [5] uses coupling resonances and a special ring to change the projections to subspaces. In this paper we present a new method where these constraints don't apply, because the system is non-Hamiltonian. The new method can be used to reduce the transverse emittance at the expense of the longitudinal one. In many accelerators the longitudinal emittance is artificially blown-up in order to reduce instabilities. Replacing these methods by a transverse-longitudinal emittance transfer presented here the transverse emittance can be reduced by a significant amount. The main advantage compared to the existing methods is the possibility to achieve not only a complete emittance exchange, but the transverse emittance can be reduced by any ratio within practical limits. The trans-

fer of emittance happens in thousands of turns and the process can be stopped, when the transverse emittance is sufficiently small, or the longitudinal emittance can not be increased further. Because of the simplicity of the new method existing accelerator rings might be modified to use it. Description of the new method is given with a possible solution to generate the transverse quadrupole electric field. We present results of numerical simulations both with single particles and with bunch of particles.

II. THE BASIC IDEA

Let's consider a particle circulating in a storage ring, that contains at least one accelerating cavity with some RF voltage, and another RF resonator that generates a transverse quadrupole electric field. This second electric field can be given as

$$E(x, y, t) = E_g (\mathbf{i}x - \mathbf{j}y) \cos(\omega t + \phi) , \quad (1)$$

where $E_g = dE/dx$ is the gradient of the electric field in $[V/m^2]$ and \mathbf{i}, \mathbf{j} are the Cartesian unit vectors. The electric field in Eq. (1) can be derived from the vector potential, the magnetic field obtained from the same vector potential is zero.

$$A(x, y, t) = -A_g (\mathbf{i}x - \mathbf{j}y) \sin(\omega t + \phi) , \quad (2)$$

$$\mathbf{B} = \nabla \times \mathbf{A} = 0 , \quad (3)$$

$$\mathbf{E} = -\frac{d\mathbf{A}}{dt} . \quad (4)$$

The direction of the electric field points inward in the horizontal plane and points outward in the vertical plane, there is no longitudinal component. Fig. 2 and Fig. 3 might help visualize this field. Imagine a beam diverging in the horizontal plane and converging in the vertical. A positively charged particle traveling in such a beam loses kinetic energy through the RF electric field, because its motion most of the time have transverse components which are opposite of the direction of the force

*Electronic address: Lajos.Bojtár@cern.ch

acting on it. Inside the resonator the sum of the kinetic and potential energy is constant, however when the particle leaves the transfer resonator (TR from here) the potential drops to zero. That means there is an energy flow outward the system most of the time when a particle goes through the TR, which is equal to the kinetic energy loss of the particle. Please note, a vector field can be non-conservative even its curl is zero, if the field is defined on a non-simply connected domain, like a torus or a cylinder [6]. The amount of the energy loss depends on the transverse amplitude of the particle. In the accelerating cavity the particle gains or loses energy depending on its phase respect to the synchronous particle. Please note this later energy change is strictly a function of phase, while the energy change in the TR is a function of the transverse trajectory inside that field. These is no guarantee the energy flowing outward the system in the TR equals exactly the energy gain or loss in the accelerating cavity. This is an open system. The mean energy of any particle stays unchanged by the exchange with the outside world, but it can provide the necessary energy difference required for a different emittance.

It is not very usual to speak about non-Hamiltonian system in accelerator physics, when only external electromagnetic forces are applied. There is an apparent contradiction: Why the motion in each element can be described by the Hamiltonian formalism and still the system as a whole can not be? In order to describe the motion exactly in the Hamiltonian framework there must be a constant of motion, which is the sum of kinetic and potential energy (for simplicity let's consider the non-relativistic case). This constant might be not strictly valid on a fine timescale, but if it exist on a larger time scale the system can be described by the Hamiltonian formalism, at least approximately. There are two places where the kinetic energy of the particle changes. These changes must be compensated by the potential energy change, if the system is Hamiltonian. The transverse electric field requires a potential which depends on the transverse oscillation amplitudes and also on the phase. The accelerating cavity requires an other potential which is a function of the phase only. In general these two required potentials are conflicting. It is not possible to find a single potential function, which can compensate the kinetic energy change in the transverse electric field and also in the accelerating cavity. The system can not be described by the Hamiltonian formalism.

When only one constraint is present the system shows the signs of Hamiltonian system. If the transverse electric field is not present the system is Hamiltonian, that is the usual setup. Let see what happens when the accelerating cavity is off. The simulation result of this case is shown on Fig. 1. The same FODO cell was simulated which is shown on Fig. 5, with cavity off. The ellipses are fitted on phase space points in the vertical plane after each 100 turns. As the particle loses kinetic energy the optical function changes, that is why the orientation of ellipses are different. The area of the ellipses stay the

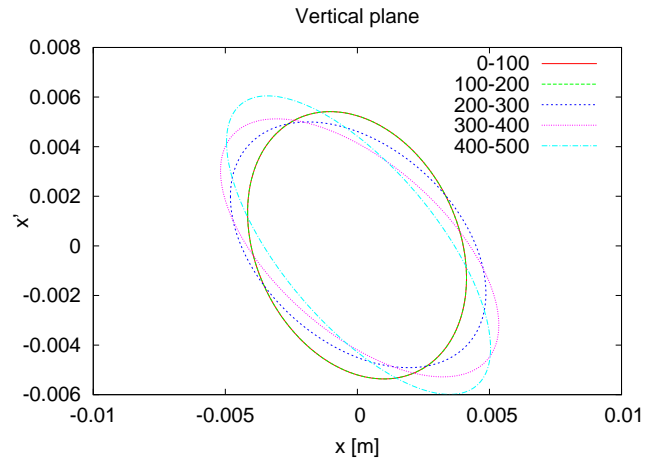


FIG. 1: Simulation with cavity off. Ellipses fitted on the vertical phase space points after each 100 turns, the points are not shown for clarity.

same, later it will be explained why. After certain time the particle slips in phase respect to the phase of the TR and will gain energy again. The particle makes complete oscillations in energy while the single particle emittance stays constant, it also means the normalized single particle emittance oscillates together with the energy. This is already not strictly Hamiltonian motion, but in a large timescale can be considered as Hamiltonian, because one can find a potential function compensating the kinetic energy oscillations. When both the cavity voltage and the transverse electric field are present it is not possible to find an appropriate potential function. The phase space plot for this case is shown on Fig. 4, as can be seen the emittance shrinks transversally and grows longitudinally.

We derive a formula for the average energy loss. It is assumed the electric field changes only a negligible amount during the passage of the particle. The result has to be corrected by a time transit factor, which can be calculated for a given case. The horizontal trajectory of the particle inside the electric field can be written as

$$x(t) = x_0 \cos(\sqrt{K_e}t) + \frac{v_{x0} \sin(\sqrt{K_e}t)}{\sqrt{K_e}}, \quad (5)$$

where

$$K_e = \frac{qE_g}{m_0\gamma}, \quad (6)$$

and L is the length of TR, x_0 is the horizontal position of the particle at $t = 0$, v_{x0} is the horizontal velocity at $t = 0$. We have chosen $t = 0$ when the particle is at half way between the entry and the exit of the TR. The energy change is equal to the potential difference between the entry and the exit point of the particle. The E field at a given time t at the position of the particle is

$$E_x = E_g x(t), \quad (7)$$

and the potential is

$$U = - \int E_x dx = -\frac{1}{2} E_g x(t)^2 . \quad (8)$$

Using the trajectory Eq. (5) and setting $t = -L/(2v_z)$, the potential of the point where the particle enters the TR is

$$U_{\text{entry}} = -\frac{1}{2} E_g \left(x_0 \cos \left(\frac{\sqrt{K_e} L}{2v_z} \right) - \frac{v_{x0} \sin \left(\frac{\sqrt{K_e} L}{2v_z} \right)}{\sqrt{K_e}} \right)^2 . \quad (9)$$

Similarly setting $t = L/(2v_z)$ the potential of the exit point is

$$U_{\text{exit}} = -\frac{1}{2} E_g \left(x_0 \cos \left(\frac{\sqrt{K_e} L}{2v_z} \right) + \frac{v_{x0} \sin \left(\frac{\sqrt{K_e} L}{2v_z} \right)}{\sqrt{K_e}} \right)^2 . \quad (10)$$

The difference of entry and exit potentials give the kinetic energy change of the particle, which is

$$\Delta U_h = U_{\text{exit}} - U_{\text{entry}} = -E_g \frac{v_{x0} x_0 \sin \left(\frac{\sqrt{K_e} L}{v_z} \right)}{\sqrt{K_e}} . \quad (11)$$

Let be $x'_0 = v_{x0}/v_z$ at $t=0$, then

$$\Delta U_h = -E_g \frac{v_z x_0 x'_0 \sin \left(\frac{\sqrt{K_e} L}{v_z} \right)}{\sqrt{K_e}} . \quad (12)$$

The average energy change per turn can be obtained by integrating the energy loss along the phase space ellipse. Let be α and β twiss parameters at the middle of the TR. In many turns the points x_0 and x'_0 give an ellipse in the phase space. The parametric equation of the ellipse is

$$x_0 = \sqrt{\epsilon_h \beta_h} \cos(\theta) , \quad (13)$$

$$x'_0 = -\frac{\sqrt{\epsilon_h}}{\sqrt{\beta_h}} (\alpha_h \cos(\theta) + \sin(\theta)) . \quad (14)$$

Substituting Eq. (13) and Eq. (14) into Eq. (12)

$$\begin{aligned} \Delta U_{avh} &= -E_g \frac{v_z \sin \left(\frac{\sqrt{K_e} L}{v_z} \right)}{2\pi \sqrt{K_e}} \int_0^{2\pi} x_0 x'_0 d\theta \\ &= E_g \frac{\epsilon_h v_z \alpha_h \sin \left(\frac{\sqrt{K_e} L}{v_z} \right)}{2\sqrt{K_e}} . \end{aligned} \quad (15)$$

Following the same procedure in the vertical plane and taking the two planes together the average energy change per turn in electron volts is

$$\begin{aligned} \Delta U_{av} &= \frac{E_g v_z}{2\sqrt{K_e}} \epsilon_h \alpha_h \sin \left(\frac{\sqrt{K_e} L}{v_z} \right) \\ &\quad - \frac{E_g v_z}{2\sqrt{K_e}} \epsilon_v \alpha_v \sinh \left(\frac{\sqrt{K_e} L}{v_z} \right) . \end{aligned} \quad (16)$$

A particle with some transverse oscillation averaged over many turns loses or gains energy depending on the sign of E_g and the optical parameter α . The energy change is proportional to α and ϵ . In order to see how the emittance can be reduced in the transverse planes we consider a simplified case, where the particle moves with a non-relativistic speed. That simplification allows us to solve the equation of motion in the transverse electric field exactly, analytically. It is important to have an exact solution, because the effect we are interested in is small and it accumulates in thousands of turns. We obtain the equation of motion in the electric field as

$$\frac{d(m\mathbf{v})}{dt} = q \mathbf{E} . \quad (17)$$

Considering only the horizontal plane, the equation of motion is

$$\frac{d^2 x}{dt^2} - \frac{qE_g}{m} x = 0 . \quad (18)$$

Solving the differential equation, one obtains a transfer matrix for the TR.

$$M_h = \begin{vmatrix} \cos(\phi) & \frac{1}{\sqrt{|K_e|}} \sin(\phi) \\ -\sqrt{|K_e|} \sin(\phi) & \cos(\phi) \end{vmatrix} \quad (19)$$

Where $\phi = \sqrt{|K_e|} L/v_z$, and L is the length of the TR. This transfer matrix has the same form as the transfer matrix of the magnetic quadrupole, however this matrix is exact, while in the case of magnetic quadrupole it is a linear approximation. The determinant of the matrix above is 1, meaning the transformation preserves the horizontal phase space area. That is the reason why the ellipses have the same area on Fig. 1. As the particle loses energy at each passage of the transverse electric field explained already above, the particle going to regain the energy loss in the accelerating cavity. Due to this re-acceleration the transverse emittance in both planes will decrease by a factor $(p_0 - \Delta p)/p_0$, where $\Delta p = \Delta U_{av}/v_z$ in $[eV/c]$ and ΔU_{av} can be calculated by Eq. (16). That is one mechanism, however this isn't the only one involved. The equation of motion inside a magnetic quadrupole is nonlinear. The 6D emittance of a bunch traveling through a magnetic quadrupole stays constant, but not the projections to the horizontal, vertical and longitudinal planes. That can be seen if one calculates the Jacobian matrix of the transformation due

to a magnetic quadrupole and diagonalize it. In the diagonalized matrix there is a complex conjugate pair for each plane. The product of a pair is a real number which is different from 1 by a small amount, that means emittance increase if the product is bigger than 1, or decrease if it is smaller. The product of all diagonal entries is 1, because the 6D phase space volume stays constant in a magnetic quadrupole. In an accelerator having magnetic quadrupoles only, this exchange of phase space volume between the planes has no net effect, because there is as much as flow in one direction as the opposite in a complete period of betatron oscillation. In the case of TR the diagonalized Jacobian matrix consists of complex conjugate pairs whose product is 1 for each transverse planes. In an accelerator containing both magnetic quadrupoles and TR's placed as it is described above, there is a net transfer of phase space volume from the transverse planes towards the longitudinal, because the TR cause some phase advance of the betatron oscillation, but no emittance change in the transverse planes, so there will be more phase space volume transferred from the transverse plane toward the longitudinal one, than from the longitudinal towards the transverse in a complete period of the betatron oscillation.

III. TRANSVERSE ELECTRIC FIELD GENERATION

It isn't an aim of this paper to present a detailed design of the apparatus, but to demonstrate that the method is feasible and the electric field in Eq. (1) can be practically realized. The electric field is similar to the field of an RFQ, with the difference, it has no longitudinal component. The physical structure of the TR similar to the structure of RFQ's, but it has no vane modulation. The frequency of the TR must be relatively low, because during the time a bunch travels through the TR the RF voltage should not change sign. If the RF voltage changed sign, some particles in the bunch would loose energy, and others would gain. One possible structure is described in [7]. This type of design has the advantage of having a resonant frequency inversely proportional to its length. The RFQ in [7] without vane modulation has been modeled with Microwave Studio [8]. The structure is shown on Fig. 2. The diameter of the cylinder is 19 cm, it's length is 50 cm, the diameter of the rods are 1.9 cm. The electric field between the rods has the best linearity if the ratio between the radius of the rods and their distance from the center is 1.4115. With these dimensions the structure resonates at 58 MHz, which limits the maximum bunch length to 8.63 ns, that is rather short. The frequency can be lowered making the structure longer. There are RFQ's working in the 10 MHz range [9]. Fig. 3 shows the electric field from a view point on the beam axis. The magnetic field is located outside the rods and has no effect on the beam.

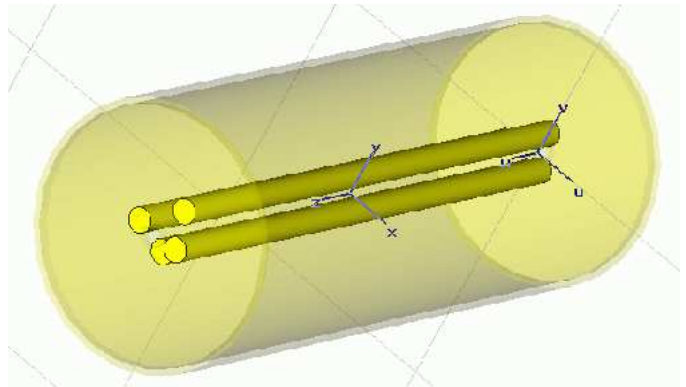


FIG. 2: One possible design of a TR to generate quadrupole electric field

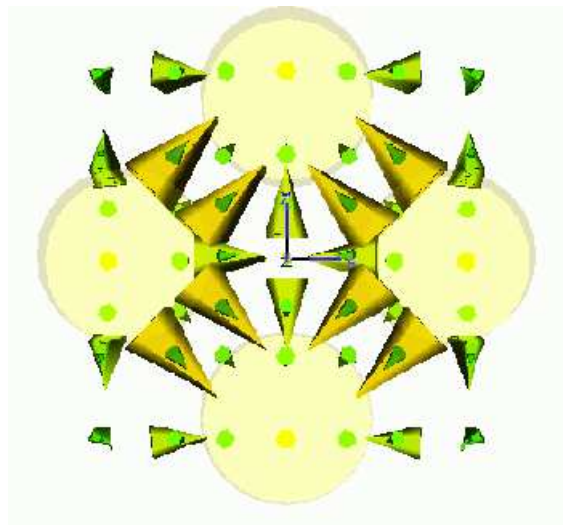


FIG. 3: The electric field between the the rods.

IV. SIMULATIONS

A. The method

The most commonly used accelerator simulation tools are symplectic integrators. These have the nice property of keeping the numerical errors bounded, even after a very large number of turns. This advantage come from the fact they are used for simulations of Hamiltonian systems. In our case the system is non-Hamiltonian and there is no advantage of using a symplectic integrator. Classical methods like Runge-Kutta-Cash-Karp with automatic step size adjustment found to be precise enough for the number of turns simulated, in our case a few tens of thousands. A Java code has been developed from scratch to perform the simulation. The source code is freely available from the author at request. The effect we are interested in accumulates over thousands of turns, so it was important to avoid any approximations and having a full understanding what the code does. Six

type of elements has been implemented: Sector bending, magnetic quadrupole, magnetic sextupole, RF accelerating cavity, drift space and the TR. All simulations used some combination of these elements. All elements were treated with the hard-edge model, no fringe field effects were included. The numerical precision has been verified by performing time reversed tracking. The initial conditions of the forward tracking has been re-obtained with 6-7 digit precision after time reversed tracking (20000 traversals of the FODO cell).

1. Sector bending

The trajectory in the sector bending is treated in a geometric way in a global coordinate system, where the x, y plane is the bending plane and the z coordinate is the vertical one. The particle arriving in the bending moves on a circle with a radius determined by

$$\rho = \frac{p_{xy}}{Bq} , \quad (20)$$

where

$$p_{xy} = \gamma m_0 \sqrt{v_x^2 + v_y^2} . \quad (21)$$

The center of the circle lies on the line perpendicular to the particle's trajectory at the entry. Then the intersection of the trajectory circle and the exit edge is calculated, that gives the x and y coordinates at the exit. The v_x, v_y velocity components are rotated in a global coordinate system by the angle extent of the arc between the entry and the exit points, v_z is unchanged. The z coordinate at the exit is calculated as $z = z_0 + v_z L / v_{xy}$, where L is arc length between the entry and the exit points.

2. Quadrupole

The global coordinates and velocities are transformed to a local one, then the trajectory is calculated by solving the equations of motion numerically, and finally the local coordinates and velocities are transformed back to the global coordinate system. In the local coordinate system x stands for the horizontal position y for the vertical and z for the longitudinal. The equation of motion is obtained as

$$\begin{aligned} \frac{d\mathbf{p}}{dt} &= q(\mathbf{B} \times \mathbf{v}) , \\ \mathbf{B} &= \{B_g x(t), B_g y(t), 0\} , \\ B_g &= \frac{B_x}{dx} , \end{aligned} \quad (22)$$

which gives

$$\begin{aligned} x''(t) + K_m x z'(t) &= 0 , \\ y''(t) - K_m y z'(t) &= 0 , \\ z''(t) - K_m (x x'(t) - y y'(t)) &= 0 , \end{aligned} \quad (23)$$

with

$$K_m = \frac{B_g q}{m_0 \gamma} . \quad (24)$$

Please note there is a longitudinal component of the force, which is missing in the usual approximative formalism. The independent variable is time. The precise time when the particle exits the quadrupole isn't known for advance, it is found by successive approximations.

3. Sextupole

The procedure is similar to the quadrupole but the magnetic field is

$$\mathbf{B} = \{B_g x(t) y(t) , \frac{1}{2} B_g (x(t)^2 - y(t)^2) , 0\} , \quad (25)$$

leading to

$$\begin{aligned} x''(t) + \frac{K_m}{2} z'(t) (x(t)^2 - y(t)^2) &= 0 , \\ y''(t) - K_m z'(t) x(t) y(t) &= 0 , \\ z''(t) - \frac{K_m}{2} ((x(t)^2 - y(t)^2) x'(t) - 2x(t) y(t) y'(t)) &= 0 . \end{aligned} \quad (26)$$

4. Cavity

The longitudinal component of the momentum is increased in a single step at the middle of the cavity's physical length, by the amount which corresponds to the energy change: $\Delta E = V_0 \sin(\omega t + \phi)$ in [eV]. The spaces before and after the middle point are treated as drift space. The transverse velocities are modified to keep the transverse momentum unchanged.

5. Transverse quadrupole electric field

The procedure is similar to the magnetic quadrupole but the equation of motion is derived starting with $d\mathbf{p}/dt = \mathbf{E}q$ using Eq. (1) and taking into account the γ is changing during the transfer, we obtain

$$\begin{aligned} x''(t)\gamma(t) + x'(t)\xi(t) - \frac{E_g q}{m_0} \cos(\phi + \omega t)x(t) &= 0 , \\ y''(t)\gamma(t) + y'(t)\xi(t) + \frac{E_g q}{m_0} \cos(\phi + \omega t)y(t) &= 0 , \\ z''(t)\gamma(t) + z'(t)\xi(t) &= 0 , \end{aligned} \quad (27)$$

where

$$\xi(t) = \frac{\gamma(t)^3 (x'(t)x''(t) + y'(t)y''(t) + z'(t)z''(t))}{c^2} . \quad (28)$$

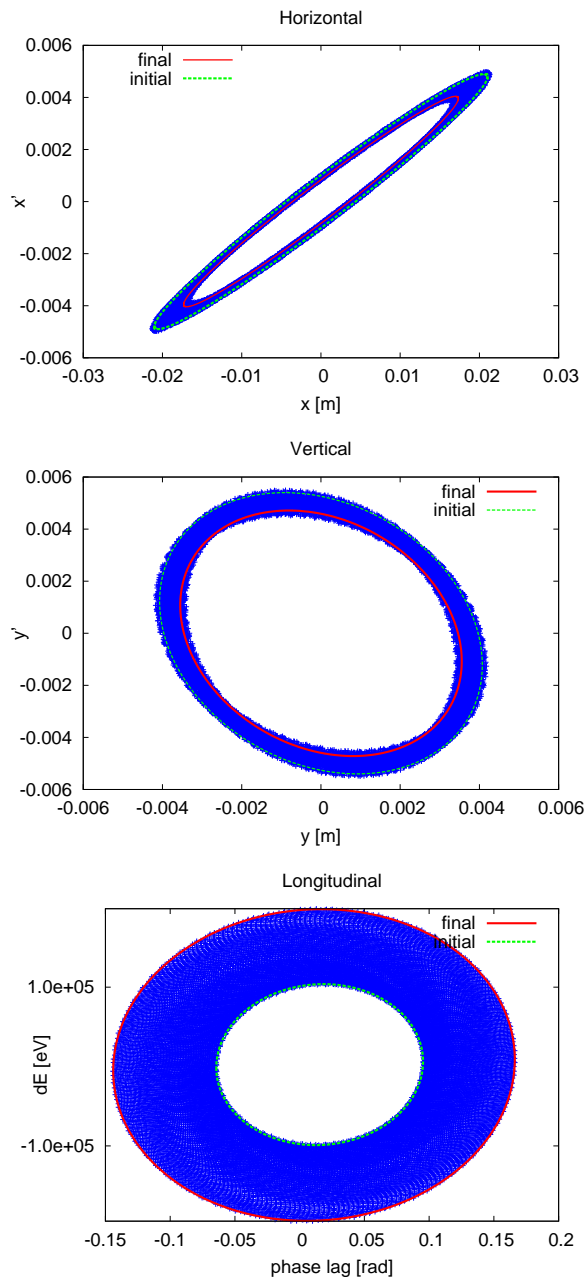


FIG. 4: Phase-space plots at the exit of the horizontally defocusing TR. The green ellipses is fitted onto the first 100 points and the red ones fitted onto the last 100. The number of "turns" (traversals) is 20000.

The same equation was derived from the relativistic Lagrangian as a cross check.

B. Single particle tracking results

There are a large number of possible settings even with the simplest approach, described below. Many combinations of these settings has been tried. The system shows

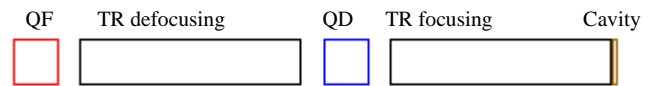


FIG. 5: FODO cell, containing a focusing (red), a defocusing (blue) quadrupole, two TR's (black) and a cavity (braun).

quite complicated behavior in some cases. First we take a simple approach, simulating regular FODO cells aligned in a straight line. The TR can be useful in circular accelerators only, because the beam must go through thousands of times to achieve a significant emittance transfer, despite of this we can gain insight, because the two case isn't much different if the TR is put into a circular machine where the dispersion is zero. Fig. 5 shows the cell, its length is 7m, the length of the quadrupoles are 0.5m the length of the TR's are 2.5m, cavity length (gap) is 5cm. Fig. 4 shows position-angle coordinates in the horizontal and vertical phase-space, and ΔE [eV] and phase lag [rad] coordinates in the longitudinal one. These are the results of a simulation where a single particle traveled through the FODO cell 20000 times with the following settings: The phase of the TR's is adjusted such that a synchronous particle arrives at the middle of the TR's when the RF electric field has its maximum, $\pm 6MV/m$, its frequency is L_{fodo}/v_s . Focusing quadrupole strength $k=1.122$, defocusing $k=-1.1$. The different strength of quadrupoles are necessary to have a different tune in the transverse planes. Cavity voltage is 10^5 [V], initial single particle emittances are $\epsilon_h = 21.4$ [mm mrad], $\epsilon_v = 21.4$ [mm mrad], $\epsilon_L = 9.88 \times 10^{-5}$ [eVs]. The final emittances are $\epsilon_h = 14.4$ [mm mrad], $\epsilon_v = 16.3$ [mm mrad], $\epsilon_L = 3.7 \times 10^{-4}$ [eVs]. The single particle emittances were calculated from an ellipse fitted on points in the phase space by least square fitting [10].

Let be R_H the ratio between the initial and final single particle horizontal emittance and similarly R_V for the vertical and R_L for the longitudinal. In simulation runs with different parameters, it has been found that

$$R_H^2 R_V^2 R_L = 1. \quad (29)$$

There are some exception from this relation. When the horizontal and vertical tunes are the same, the product $R_H^2 R_V^2 R_L$ depends on the initial phase difference between the horizontal and vertical betatron motion. This is because the initial phase difference says constant, due to the equal betatron tunes. In practice the tunes are never exactly the same. An other exception is when the amplitude of the betatron oscillation is very large, and there is an slow emittance oscillation between the two transverse planes, even when the TR's are off.

The rate of change of the longitudinal single particle emittance has a strong correlation with dU/dE , which is the average energy loss (in the TR's) dependence on the energy, just like in the case of synchrotron radiation damping of electrons. Fig. 6 shows dU/dE vs. N , on a

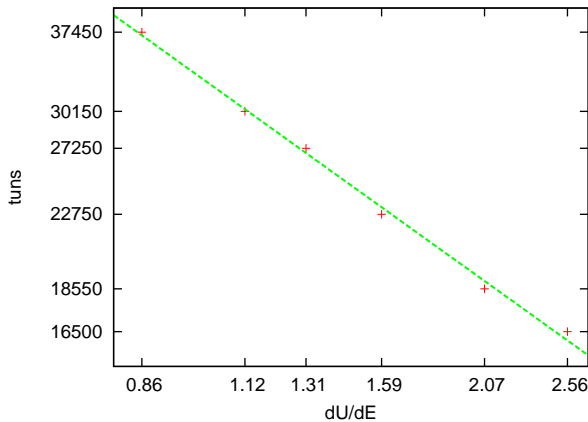


FIG. 6: Number of turns needed to reduce transverse emittance by a factor 2, versus dU/dE plotted on a log-log scale

log-log scale, where N is the number of turns needed to reduce the transverse emittance by half. It can be seen from Eq. (16), the value of dU is dependent on the optical function α . The closer the quadrupole strength gets to the upper limit in the "necktie" stability diagram of the FODO cell, the more efficient the transfer between transverse and longitudinal planes becomes. As one gets close to the stability limit, the optical function α becomes very sensitive to small changes in energy, and the value of dU/dE becomes bigger, meaning faster changes of emittances. TABLE I shows the result of several runs with different quadrupole strengths (k). The initial emittances are chosen such that the average energy loss per turn stays the same, 2 KeV for each k value. Then the number of traversals of the FODO cell, lets call them "turns", necessary to achieve a ratio 2 between the initial and final transverse emittances is determined. It can be seen, the number of turns is getting smaller as k is increasing. The longitudinal emittance puts the limit how close the stability limit can be approached. The last column of TABLE I is the energy loss dependence on the energy. It has been calculated from Eq. (16), by substituting α_h and α_v values at the nominal energy E_0 and some slightly different α values at $E_0 + \Delta E$, then

$$\frac{dU}{dE} = \frac{\Delta U_{av}(E_0 + \Delta E) - \Delta U_{av}(E_0)}{\Delta E}. \quad (30)$$

The α values were calculated by MADX [11] at the nominal k and at a slightly different k due to the ΔE energy deviation.

Simulations has been tried at different energies. The speed of emittance transfer stays constants if the focusing strength of the quadrupoles and the TR's kept the same. The limiting factor to make the method work on higher energy is the gradient of the electric field in the TR. In RFQ's the maximum electric field gradient is in the order of 30 MV/m. Taking this limitation into

k	ϵ_{hi}	ϵ_{vi}	ϵ_{li}	ϵ_{hf}	ϵ_{vf}	ϵ_{lf}	turns	ΔE	dU/dE
1.1	27.43	27.53	1	18.19	20.67	4.02	16500	27.32	2.56
1.09	29.3	29.3	1	19.67	21.9	3.96	18550	30.7	2.07
1.07	32.8	32.5	1	22.27	24	3.95	22750	37.9	1.59
1.05	35.4	35.1	1	24.2	25.7	3.99	27250	45	1.31
1.035	38.4	36.6	1	26.2	26.9	4.01	30150	50.2	1.12
1.0	41.7	41.2	1	28.8	29.9	4.02	37450	62.05	0.86

TABLE I: Emittance transfer with different quadrupole strengths. Transverse emittances are in [mm mrad] longitudinal ones are in [10^{-4} eVs], ΔE [MeV] is the total energy loss in TR's, dU/dE [10^{-4}] is the energy loss (in TR's) dependence on energy ϵ_{hi} , ϵ_{vi} , ϵ_{li} are the initial emittances and ϵ_{hf} , ϵ_{vf} , ϵ_{lf} are the final ones.

account, the upper energy limit of the method is around a few GeV, depending on how long time is available for the process.

A few numerical experiment was performed with a circular machine too. This type of experiment requires far more work to set up and at the moment only a few results are obtained. The aim was to verify if something is fundamentally different from the case with a long series of FODO cells aligned in a straight line. There was no difference. The TR's were placed at a location in the machine where the dispersion is zero. The relation between emittances given by Eq. (29) still holds. A setup has been tried when, when the chromaticity was overcompensated by sextupoles, so the dU/dE changed sign. As expected the longitudinal emittance was decreasing and the transverse emittance was increasing and the relation given by Eq. (29) was still valid.

C. Bunch tracking results

Bunch tracking was performed with the same FODO cell used for single particle tracking with quadrupole strength $k_{QF} = 1.1$, $k_{QD} = 1.122$ at 300 MeV/c. A 6D Gaussian distribution has been generated and used as initial conditions for 10000 single particle tracking. The number of turns was 10000. Fig. 7 shows the distributions in the horizontal, vertical and longitudinal planes. The red crosses correspond to the initial points in the phase spaces and the greens are the final ones. It can be seen the transverse emittances are reduced and the longitudinal one is increased. Also the distributions has changed, in the transverse planes the edges become much better defined, in the longitudinal one it has been smeared out. In the longitudinal plane there are points very far from the mean. These are the points which were far from the mean in the transverse planes and also in the longitudinal planes already in the initial distribution. Since the probability for an initial point being in the tail of the distribution both in the transverse and longitudinal planes is small, there are relatively few of them. The blue ellipse marks the 2σ limit, 95 % of the particles are

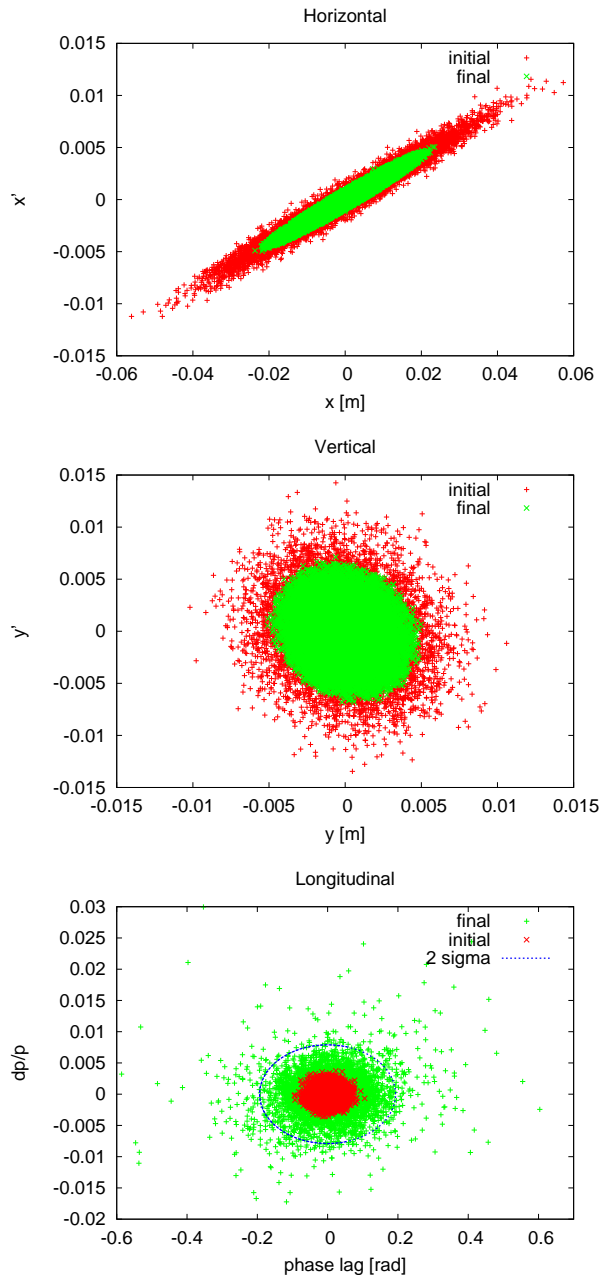


FIG. 7: Distributions of 10000 points in phase-space before and after 10000 turns.

inside.

Emittances were calculated before and after tracking by the method given by Wolski [12]. His method can be used even there are correlations between the planes. Here is a short summary. The beam Σ matrix is defined as $\Sigma_{ij} = \langle (X_i - \bar{X}_i)(X_j - \bar{X}_j) \rangle$, where $X^T = (x, x', y, y', \tau, \delta)$ and a matrix S defined as

$$S = \begin{pmatrix} 0 & 1 & 0 & 0 & 0 & 0 \\ -1 & 0 & 0 & 0 & 0 & 0 \\ 0 & 0 & 0 & 1 & 0 & 0 \\ 0 & 0 & -1 & 0 & 0 & 0 \\ 0 & 0 & 0 & 0 & 0 & 1 \\ 0 & 0 & 0 & 0 & -1 & 0 \end{pmatrix}.$$

Then the eigenvalues of ΣS are $\pm i\epsilon_x$, $\pm i\epsilon_y$, $\pm i\epsilon_z$. The brackets $\langle \rangle$ mean averaging over all particles. The result of the emittance calculations are in TABLE II. As it can be seen the 6D rms emittance is much bigger after tracking. This is possible even in a Hamiltonian system. Please note, since the system is reversible in time the 6D rms emittance can also decrease, however this is not very useful since the motion is unstable. Starting from a Gaussian distribution it would lead very quickly to severe losses. The first row shows the case when all particles are included in the calculation. The second row shows the case when only those particles were taken into account, which are inside 2σ in the longitudinal plane. With a given longitudinal emittance increase budget, better to allow some particle to be lost. With only 5% of the highest amplitude particles in the longitudinal plane scraped away, the ratio between transverse ϵ decrease and longitudinal ϵ increase improves significantly.

σ	ϵ_{hi}	ϵ_{vi}	ϵ_{li}	ϵ_{hf}	ϵ_{vf}	ϵ_{lf}
all inc.	10.02	9.92	0.245	5.79	4.74	1.92
2σ	9.44	9.3	0.228	5.6	4.58	1.22

TABLE II: Rms emittances before and after tracking. Transverse emittances (1σ) are in [mm mrad] longitudinal ones are in [10^{-4} rad].

V. SUMMARY AND OUTLOOK

An accelerator containing a quadrupole transverse RF field is a non-Hamiltonian system. Such a field can be used for transfer emittance between the transverse and longitudinal planes. One possible generation of the field was presented. A formula for the average energy loss in the TR's was derived. Single particle simulations showed that the relation between the transverse and longitudinal single emittance ratios (the ratio between initial and final emittances) is $R_H^2 R_V^2 R_L = 1$. Strong correlation was found between the speed of the emittance transfer and the average energy loss dependency on energy. Bunch tracking result suggest the method might lead to significant transverse emittance decrease in accelerators. Using the method at higher energies getting increasingly difficult, but in the few GeV range the method expected to work. In the CERN PS machine there is about a factor 4 longitudinal blow-up at 3.5 GeV in order to avoid

instabilities. It might be possible to replace that blow-up by the method presented here, gaining a factor 2-4 in the transverse planes. There are lots of possibility for further work. A more analytical approach might give a

deeper insight how the emittance transfer actually happens. These results strongly suggest the method can be put in practical use.

-
- [1] M. Cornacchia and P. Emma, Phys. Rev. ST Accel. Beams **5**, 084001 (2002).
- [2] P. Emma, Z. Huang, K.-J. Kim, and P. Piot, Phys. Rev. ST Accel. Beams **9**, 100702 (2006).
- [3] *Conservation of Phase Space in Hamiltonian Systems and Particle Beams, in Perspectives in Modern Physics* (R.E.Marshak, 1966).
- [4] K. Kim and A. Sessler, AIP Conf. Proc. **821**, 115 (2006).
- [5] H. OKAMOTO, K. KANETA, and A. M. SESSLER, Journal of the Physical Society of Japan **76**, 074501 (20070715), ISSN 00319015, URL <http://ci.nii.ac.jp/naid/110006350760/en/>.
- [6] *Irrotational vector field*, URL http://en.wikipedia.org/wiki/Irrotational_vector_field.
- [7] I. Moretti, Alfred (Downers Grove (1985), URL <http://www.freepatentsonline.com/4494040.html>.
- [8] G. CST GmbH, Budinger Strasse D-64289 Darmstadt, *Cst microwave studio*.
- [9] R. Kaye, K. Shepard, B. Clift, and M. Kedzie, Particle Accelerator Conference, 1999. Proceedings of the 1999 **1**, 524 (1999).
- [10] A. W. Fitzgibbon, M. Pilu, and R. Fisher, icpr **01**, 253 (1996), ISSN 1051-4651.
- [11] *Madx*, URL <http://mad.web.cern.ch/mad/>.
- [12] A. Wolski, Phys. Rev. ST Accel. Beams **9**, 024001 (2006).